Analysis of entropy generation in an inclined channel flow containing two immiscible micropolar fluids using HAM

Received 3 September 2015
Revised 18 December 2015
Accepted 21 December 2015

J. Srinivas
Department of Mathematics, National Institute of Technology Meghalaya, Meghalaya, India
J.V. Ramana Murthy
Department of Mathematics, National Institute of Technology Warangal, Telangana, India, and
Ali J. Chamkha
Mechanical Engineering Department, Prince Mohammad Bin Fahd University, Al-Khobar, Kingdom of Saudi Arabia

Abstract

Purpose – The purpose of this paper is to examine the flow, heat transfer and entropy generation characteristics for an inclined channel of two immiscible micropolar fluids.

Design/methodology/approach – The flow region consists of two zones, the flow of the heavier fluid taking place in the lower zone. The flow is assumed to be governed by Eringen's micropolar fluid flow equation. The resulting governing equations are then solved using the homotopy analysis method.

Findings – The following findings are concluded: first, the entropy generation rate is more near the plates in both the zones as compared to that of the interface. This indicates that the friction due to surface on the fluids increases entropy generation rate. Second, the entropy generation rate is more near the plate in Zone I than that of Zone II. This may be due to the fact that the fluid in Zone I is more viscous. This indicates the more the viscosity of the fluid is, the more the entropy generation. Third, Bejan number is the maximum at the interface of the fluids. This indicates that the amount of exergy (available energy) is maximum and irreversibility is minimized at the interface between the fluids. Fourth, as micropolarity increases, entropy generation rate near the plates decreases and irreversibility decreases. This indicates an important industrial application for micropolar fluids to use them as a good lubricant.

Originality/value – The problem is original as no work has been reported on entropy generation in an inclined channel with two immiscible micropolar fluids.

Keywords HAM, Bejan number, Entropy generation number, Immiscible fluids, Micropolar fluid

Paper type Research paper

Nomenclature

Be	Bejan number	$\overline{\mathbf{h}}$	heat flux ($\mathrm{W\,m^{-2}}$)
Br	Brinkman number	k_1, k_2	thermal conductivity of the fluid in Zones I, II, W/mK
Br/Ω	viscous dissipation parameter		
D	deformation tensor ($\mathrm{T^{-1}}$)	$\overline{\ell}$	body couple per unit mass ($\mathrm{L^5\,T^{-1}}$)
d_{ij}	components of the strain		
E	specific internal energy (J)	m_{ij}	couple stress tensor ($\mathrm{N\,L^{-1}}$)
Ec	Eckert number	$\mathrm{n_\eta}$	couple stress coefficients ratio
$\overline{f}$	body forces per unit mass ($\mathrm{LT^{-2}}$)	$\mathrm{n_k}$	thermal conductivity ratio
$2h$	height of the free channel (m), (L)	$\mathrm{n_\mu}$	viscosity ratio

International Journal of Numerical Methods for Heat & Fluid Flow
Vol. 26 No. 3/4, 2016
pp. 1027-1049

0961-5539
DOI 10.1108/HFF-09-2015-0354

n_ρ	density ratio
Nf_i	entropy generation due to viscous dissipation ($kg\,m^2\,s^{-2}\,K^{-1}$)
Ns_i	dimensionless total entropy generation number
Ny_i	entropy generation due to transverse conduction
Nu	Nusselt number
P	pressure, ($N\,m^{-2}$), ($ML^{-1}\,T^{-2}$)
Pr	Prandtl number
$\overline{q}$	velocity vector (ms^{-1}), ($L\,T^{-1}$)
Re	Reynolds number
s_1, s_2	couple stress parameters
$(S_i)_G$	entropy generation rate ($W\,m^{-3}\,K^{-1}$)
$(S_1)_{G,\,C}$	characteristic entropy transfer rate
T_1, T_2	temperatures, (K)
u	dimensionless velocity in X-direction
X, Y	space co-ordinates (m), (L)

Greek symbols

α, β, γ	gyro-viscosity coefficients (ML^4)
δ_{ij}	Kronecker delta
ΔT	temperature difference ($T_{II}-T_I$), (K)
τ_{ij}	stress tensor ($N\,m^{-2}$), ($M\,L\,T^{-2}$)
ε_{ijk}	Levi-Civita symbol or permutation symbol
λ, μ, κ	viscosity coefficients ($Kg\,m^{-1}\,s^{-1}$), ($ML^{-1}\,T^{-1}$)
η, η'	couple stress viscosity coefficients
$\overline{v}$	micro-rotation (T^{-1})
Ω	dimensionless temperature difference
Φ	dissipation function ($L^2\,T^{-3}$)
ϕ	irreversibility distribution ratio
ρ	density ($Kg\,m^{-3}$), (ML^{-3})
θ_1, θ_2	non-dimensional temperatures (K)

Subscripts

1	fluid in Zone I
2	fluid in Zone II

1. Introduction

In recent years, the analysis of heat transfer has been attracting more and more attention of researchers because heat transfer improvement is very important for many industrial applications and the reduction of energy consumption. The energy-related engineering systems are designed and their performance is evaluated primarily by using the energy balance deduced from the first law of thermodynamics. Engineers and scientists have been traditionally applying the first law of thermodynamics to calculate the enthalpy balances for more than a century to quantify the loss of efficiency in a process due to the loss of energy. However, in recent years the second law analysis, hereinafter called the exergy analysis of available energy analysis, of energy systems has more and more drawn the interest of engineers and the scientific community. The application of exergy analysis in engineering systems is very useful because it provides quantitative information about irreversibilities and exergy losses in the system. In this way, the thermodynamic efficiency can be quantified and poor efficiency areas can be identified, so that systems can be designed and operated more efficiently. The exergy concept has gained considerable interest in the thermodynamic analysis of thermal processes and plant systems since it has been seen that the first law analysis has been insufficient from an energy performance stand point. Therefore the use of the exergy analysis of thermodynamic systems has become an essential tool for system design and thermal conduction and convection. The exergy analysis is one of the best tools for improving the performance of engineering processes involving heat transfer. It examines the irreversibility due to fluid flow and heat transfer in terms of the entropy generation rate. The second law of thermodynamics provides a general and unique way of optimizing the design of thermal-fluid devices by minimizing the sum of thermal and frictional entropy generation rates. A set of optimal operating and design conditions is obtained that minimizes the irreversibility's in the system. Accurate estimation of the

entropy generation plays an important role in the design and development of thermo-fluid components such as heat exchangers, turbines, pipe networks, pumps, energy storage systems and electronic cooling devices. Bejan (1982, 1996) focussed on the different effective factors behind the entropy generation in thermal systems, where destruction of available work of a system occurs during the generation of entropy. Bejan (1979) presented the second law aspect of heat transfer using various forced convection problems. He established the concept of entropy generation number, irreversibility distribution ratio. Later on, many investigators are interested to determine the entropy generation and Bejan profiles for different geometric arrangements, flow situations and thermal boundary conditions. Several works on entropy generation minimization have appeared in the open literature (Baytas, 2000; Havzali *et al.*, 2008).

The flow and heat transfer of immiscible fluids in inclined channels are of special importance in the petroleum extraction and transport problems. The reservoir rock of oil field contains many immiscible fluids in its pores. A portion of the pores contains water and the rest contains oil or gases or both. The immiscible flows in crude oil transport were studied experimentally by Bakhtiyarov and Siginer (1997). Chamkha (2000) reported analytical solutions for flow of two immiscible fluids in porous and non-porous parallel-plate channels. Later on, he examined the oscillatory flow and heat transfer in two immiscible viscous fluids analytically (Chamkha, 2004). The inclined channel flow with heat transfer has attracted the attention of many researchers due to its numerous applications in thermal engineering and industries. Starting from petroleum drilling equipment to various industrial exchanger systems, this type of geometry can be observed. Malashetty and Umavathi (1997) investigated MHD two-phase flow and heat transfer in an inclined channel. In another paper, Malashetty *et al.* (2004) have studied the flow and heat transfer in an inclined channel containing fluid and porous layers. In recent years, the fluid flow and entropy generation in two immiscible fluids in an inclined/horizontal channel has received considerable attention by researchers. Komurgoz *et al.* (2010) studied thermal analysis for an inclined channel containing porous-fluid layers by using the differential transform method. Kiwan and Khodier (2011) discussed natural convection heat transfer in an open-ended inclined channel-partially filled with porous media. Other related work on various aspects of the problem under consideration can be found in Umavathi *et al.* (2005a, b, c, d, 2006, 2008, 2009a, b, 2010, 2012, 2014) and Kumar *et al.* (2010).

Many significant fluids which exhibit couple stress effects do not obey Newtonian law. Such fluids are called micropolar fluids and the constitutive equations of these fluids were proposed by Eringen (1966, 2001). Not only does a micropolar fluid sustain body forces and the usual (Cauchy) stress tensor as simple Newtonian fluids do, but it also sustains body couples and the couple stress tensor; furthermore, the stress tensor is non-symmetric in a micropolar fluid. The additional effects arise from the presence of microscopic aciculate elements in a micropolar fluid-whereby micropolar-fluid motion has six degrees of freedom, three more than of a simple Newtonian fluid-because the length scale of motion is comparable to the length scale of the aciculate elements. Micropolar fluids are known to occur in nature and are also of scientific importance. Typically, a micropolar fluid is a suspension of rigid or semi-rigid particles that cannot only translate but also rotate about axes passing through their centroids. Blood has often been modeled as a micropolar fluid (Turk *et al.*, 1973; Misra and Ghosh, 2001), because it contains platelets, cells and other particles. Modeling granular flows as micropolar fluids, Hayakawa (2000) showed that the analytical solutions of certain boundary-value problems are in correlation with the relevant experimental results.

We can expect rigid-rod epoxies to be micropolar fluids as well, because their aciculate molecules exhibit rotation about their centroidal axes (Giamberini *et al.*, 1997; Su *et al.*, 2000). Liquid crystals and colloidal suspensions are also cited as examples of micropolar fluids (Eringen, 2001). For experimental determination of parameters of micropolar fluids one can refer to Migun (1981) and Kolpashchikov *et al.* (1983).

Motivated by the aforementioned work, in this paper, we extend the previous investigations to examine the entropy generation characteristics for an inclined channel of two immiscible micropolar fluids. The homotopy analysis method (HAM) is employed to solve the governing non-linear equations. The behavior of emerging flow parameters on the velocity, micro-rotation, temperature, entropy generation number and Bejan number is studied.

2. Mathematical formulation and governing equations

Consider the flow of two immiscible micropolar fluids between two inclined parallel plates distance $2h$ apart, extending in the axial direction. As shown in Figure 1, a coordinate system may be chosen with the origin at the center of the channel. X and Y are taken as the coordinate axes parallel and perpendicular to the channel plates, respectively. The distance $2h$ between the plates is much smaller than the length of the channel so that the flow at any point in the X-direction is the same. Fluid flow is generated due to a constant pressure gradient which acts at the mouth of the channel. The fluid in the lower zone (viscosity μ_1, density ρ_1 and thermal conductivity k_1) occupies the region ($-h \leqslant Y \leqslant 0$) comprising the lower half of the channel and this region will be referred to as Zone I. The fluid in the upper zone (viscosity μ_2, density $\rho_2 < (\rho_1)$ and thermal conductivity k_2) is assumed to occupy the upper half of the channel (i.e. ($0 \leqslant Y \leqslant h$)), and this region is called Zone II. The two walls of the channel are held at different temperatures T_I and T_{II} (with $T_I < T_{II}$) and are inclined, making an angle φ with the horizontal. The fluid properties are assumed to be constant except for density variations in the buoyancy force term. The equations for the flow with buoyancy effect due to natural convection and energy in Zones I and II (i.e. $-h \leqslant Y \leqslant h$)

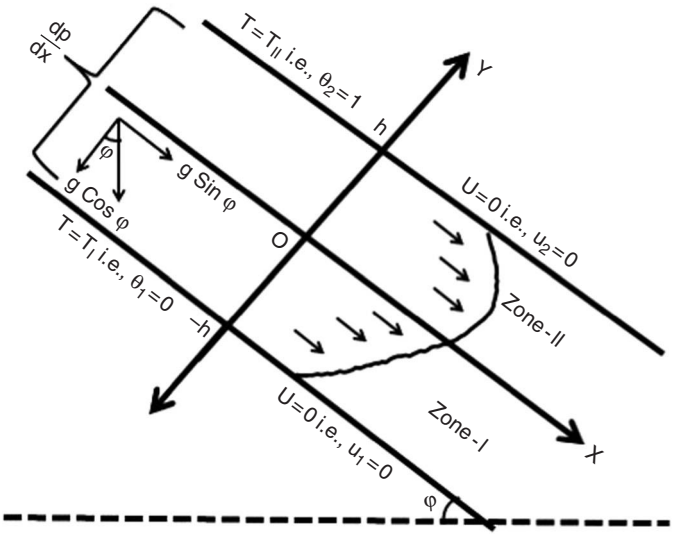

Figure 1.
The coordinate system and the geometry of the channel

are assumed to be governed by micropolar fluid flow equations as given by Eringen (1966, 2001):

$$\frac{\partial \rho}{\partial t} + \nabla \cdot (\rho \overline{q}) = 0 \tag{1}$$

$$\rho \frac{d\overline{q}}{dt} = \rho \overline{f} - \nabla P + \kappa \nabla \times \overline{v} - (\mu + \kappa) \nabla \times \nabla \times \overline{q} + (\lambda + 2\mu + \kappa) \nabla (\nabla \cdot \overline{q}) + \rho \overline{g} \tag{2}$$

$$\rho j \frac{d\overline{v}}{dt} = \rho \overline{\ell} - 2\kappa \overline{v} + \kappa \nabla \times \overline{q} - \gamma \nabla \times \nabla \times \overline{v} + (\alpha + \beta + \gamma) \nabla (\nabla \cdot \overline{v}) \tag{3}$$

$$\rho \frac{dE}{dt} = -P(\nabla \cdot \overline{q}) + \rho \Phi - \left(\nabla \cdot \overline{\mathbf{h}}\right) \tag{4}$$

where:

$$\rho \Phi = \lambda (\nabla \cdot \overline{q})^2 + 2\mu (D : D) + 4\kappa \left(\frac{1}{2} \nabla \times \overline{q} - \overline{v} \right)^2 + \alpha (\nabla \cdot \overline{v})^2 + \gamma (\nabla \overline{v} : \nabla \overline{v}) + \beta \left(\nabla \overline{v} : (\nabla \overline{v})^T \right)$$

where the vectors $\overline{q}, \overline{v}, \overline{f}$ and $\overline{\ell}$ are the velocity, micro-rotation, body force per unit mass and body couple per unit mass, respectively. P is the fluid pressure at any point. The scalar quantities ρ and j are, respectively, the density and gyration coefficient and are assumed to be constants. The material constants (λ, μ, κ) are viscosity coefficients and (α, β, γ) are gyro-viscosity coefficients. These confirm to the inequalities, $\kappa \geqslant 0$; $2\mu + \kappa \geqslant 0$; $3\lambda + 2\mu + \kappa \geqslant 0$, $\gamma \geqslant 0$; $|\beta| \leqslant \gamma$; $3\alpha + \beta + \gamma \geqslant 0$. $\overline{g}$ is the acceleration due to gravity. In the energy equation Φ is the dissipation function of mechanical energy per unit mass, D denotes the deformation tensor, i.e., $D = (1/2)(\overline{q}_{i,j} + \overline{q}_{j,i})$, E is the specific internal energy and $\overline{\mathbf{h}} = -k \ \nabla T$ is the heat flux, where k is the thermal conductivity.

Herein the velocity vector $\overline{q}$ and micro-rotation vector $\overline{v}$ are taken in the form $\overline{q} = (U(Y), 0, 0)$, $\overline{v} = (0, 0, C(Y))$.

$\overline{q} = (U(Y), 0, 0)$ satisfies the continuity Equation (1) and the governing fluid flow (neglecting body forces (except gravitational force) and body couples) and an energy equation takes the following form:

$$(\mu + \kappa) \frac{d^2 U}{dY^2} + \kappa \frac{dC}{dY} - \frac{dP}{dX} + \rho \overline{g} b (T - T_w) = 0 \tag{5}$$

$$\gamma \frac{d^2 C}{dY^2} - \kappa \frac{dU}{dY} - 2\kappa C = 0 \tag{6}$$

$$\left[\mu \left(\frac{dU}{dY} \right)^2 + \kappa \left(\frac{dU}{dY} + 2C \right)^2 + \beta \left(\frac{dC}{dY} \right)^2 \right] + k \frac{d^2 T}{dY^2} = 0 \tag{7}$$

The following dimensionless variables are used to obtain the dimensionless form of the governing equations and the boundary conditions: $x = (X/h)$, $y = (Y/h)$, $u = (U/U_o)$, $p = (P/(\rho_1 U_o^2))$, $C = ((CU_o)/h)$ and $\theta = (T - T_I)/(T_{II} - T_I)$ where U_o is the maximum velocity of the fluid in the channel.

Then, the Equations (5)-(7), in dimensionless form, in the corresponding zones are presented as follows.

Zone I: $(-1 \leqslant y \leqslant 0)$

The governing equations in Zone I are:

$$\frac{d^2u_1}{dy^2}+c_1\frac{d\mathcal{C}_1}{dy}+\frac{Gr}{Re}(1-c_1)\theta_1 Sin\varphi-Re\frac{dp}{dx}(1-c_1)=0 \tag{8}$$

$$\frac{d^2\mathcal{C}_1}{dy^2}-s_1\frac{du_1}{dy}-2s_1\mathcal{C}_1=0 \tag{9}$$

$$\frac{d^2\theta_1}{dy^2}+Br\left[\left(\frac{du_1}{dy}\right)^2+\left(\frac{c_1}{1-c_1}\right)\left(\frac{du_1}{dy}+2\mathcal{C}_1\right)^2+\delta_1\left(\frac{d\mathcal{C}_1}{dy}\right)^2\right]=0 \tag{10}$$

Zone II: $(0 \leqslant y \leqslant 1)$

The governing equations in Zone II are:

$$\frac{d^2u_2}{dy^2}+c_2\frac{d\mathcal{C}_2}{dy}+\frac{Gr}{Re}\,\frac{n_b}{n_\mu}\,(1-c_2)\;\theta_2\;Sin\varphi-\frac{1}{n_\mu}\;Re\;\frac{dp}{dx}(1-c_2)=0 \tag{11}$$

$$\frac{d^2\mathcal{C}_2}{dy^2}-s_2\frac{du_2}{dy}-2s_2\mathcal{C}_2=0 \tag{12}$$

$$\frac{d^2\theta_2}{dy^2}+\frac{Br}{n_k}\left[n_\mu\left[\left(\frac{du_2}{dy}\right)^2+\left(\frac{c_2}{1-c_2}\right)\left(\frac{du_2}{dy}+2\mathcal{C}_2\right)^2\right]+n_\beta\delta_1\left(\frac{d\mathcal{C}_2}{dy}\right)^2\right]=0 \tag{13}$$

where $Re=(\rho_1 U_o h)/\mu_1$ is the Reynolds number; $c_i=\kappa_i/(\kappa_i+\mu_i)$ $(0 \leqslant c_i<1)$, the coupling number or micropolarity parameter; $s_i=(\kappa_i h^2)/\gamma_i$, the couple stress parameter; $n_\mu=\mu_2/\mu_1$, the viscosity ratio; $Br=Ec.Pr$, the Brinkman number; $Ec=U_o^2/(c_{p_1}(T_{II}-T_I))$, the Eckert number; $Pr=(\mu_1 c_{p_1})/k_1$, the Prandtl number; $Gr=(\rho_1^2\;g\;b_1\;h^3\;(T_{II}-T_I))/\mu_1^2$, the Grashof number; $n_k=k_2/k_1$, the thermal conductivity ratio; $n_b=b_2/b_1$, the thermal expansion coefficient ratio; $n_\beta=\beta_2/\beta_1$, the couple stress coefficient ratio; and $\delta_1=\beta_1/(\mu_1 h^2)$ (i = 1, 2).

2.1 Boundary and interface conditions

A characteristic feature of a two-layer flow problem is the coupling across liquid-liquid interfaces. The liquid layers are mechanically coupled via transfer of momentum across the interfaces. Transfer of momentum results from the continuity of tangential velocity and a stress balance across the interface. To determine the velocity and micro-rotation components $u_1(y)$, $C_1(y)$, $u_2(y)$ and $C_2(y)$ in Zones I and II from (8) to (13) described above, we adopt the following boundary and interface conditions:

Zone I is constituted by the fixed lower plate given by $y=-1$ and a fluid-fluid interface defined by $y=0$. Zone II is constituted by the fluid interface given by $y=0$

and the fixed upper plate given by $y = 1$. In view of the no-slip condition on the static boundaries, we have to prescribe velocity as:

$$u_1(y) = 0 \quad \text{on } y = -1, \quad u_2(y) = 0 \quad \text{on } y = 1 \tag{14}$$

which represent the no-slip condition.

The micro-rotation vector on the boundary = angular velocity of the fluid on the boundary, i.e., $C_{wall} = (1/2)(\nabla \times \overline{q}_{wall})$. A more general condition is taken as $\mathcal{C}_{wall} = n(\nabla \times \overline{q}_{wall})$ where $0 \leqslant n \leqslant 1$ (refer Lukaszewicz, 1999, p. 31). This value of n indicates the concentration of micropolarity or interaction of fluid particles with the boundary. The case $n = 0$ indicates $\mathcal{C} = 0$ at the plates. It represents the flow of concentrated particles in which the microelements closed to the wall surface are unable to rotate (Jena and Mathur, 1981). This case is also known as strong concentration of microelements. Authors Rees and Bossom (1996) and Bhattacharyya *et al.* (2012) have used this condition. The micro-rotation vanishes on the static boundaries:

$$\mathcal{C}_1(y) = 0 \quad \text{on } y = -1, \quad \mathcal{C}_2(y) = 0 \quad \text{on } y = 1 \tag{15}$$

At the fluid-fluid interface y = 0, we assume that the velocity, micro-rotation, shear stress and couple stress components are continuous. This implies:

$$\begin{aligned} &u_1(0^-) = u_2(0^+), \quad \mathcal{C}_1(0^-) = \mathcal{C}_2(0^+), \\ &\tau_{xy1}|(0^-) = \tau_{xy2}|(0^+) \quad \text{and} \quad M_{xy1}|(0^-) = n_\beta M_{xy2}|(0^+) \end{aligned} \tag{16}$$

The last two conditions of (16) give us:

$$\tau_{xy1}|(0^-) = \tau_{xy2}|(0^+) \Rightarrow \left[\tfrac{\partial u_1}{\partial y}|(0^-) + 2c_1\mathcal{C}_1|(0^-)\right] = n_\mu\left(\tfrac{1-c_1}{1-c_2}\right)\left[\tfrac{\partial u_2}{\partial y}|(0^+) + 2c_2\,\mathcal{C}_2|(0^+)\right],$$

$$M_{xy1}|(0^-) = M_{xy2}|(0^+) \Rightarrow \frac{\partial \mathcal{C}_1}{\partial y}|(0^-) = n_\beta \frac{\partial \mathcal{C}_2}{\partial y}|(0^+). \tag{17}$$

Also to determine the temperature distributions $\theta_1(y)$ and θ_2(y), in the zones I and II described above, we adopt the following boundary and interface conditions:

(1) at the lower and upper plate boundaries the temperatures are, respectively:

$$\theta_1 = 0 \quad \text{at } y = -1 \quad \text{and} \quad \theta_2 = 1 \quad \text{at } y = 1 \tag{18}$$

(2) at the fluid interface temperature (θ) and heat flux $(\overline{\mathbf{h}})$ are continuous:

$$\theta_1 = \theta_2 \quad \text{and} \quad \frac{d\theta_1}{dy} = n_k \frac{d\theta_2}{dy} \quad \text{at } y = 0 \tag{19}$$

The solutions for u_1, $\mathcal{C}_1$, θ_1, u_2, $\mathcal{C}_2$ and θ_2 in (8)-(13) under the conditions (14)-(19) are solved by HAM.

3. The HAM solution of the problem

One of the powerful analytical techniques, namely, the HAM, has attracted special attention of researchers as it is both flexible in applying and gives sufficiently accurate results with modest effort. The method is based upon the introduction of a homotopy

parameter q which takes the values from 0 to 1. When $q = 0$, the problem under study takes a simple form which admits a closed form analytical solution for an initial guess satisfying boundary conditions. As q is increased and finally takes the value one, the exact solution to the original problem is recovered. The nice feature in this method is that it is being done entirely analytically. The HAM has been introduced and refined by Liao (1992) who has enunciated a clear treatment of the method in his classical work (Liao, 2003). The HAM relies on two other auxiliary quantities, a convergence controlling parameter h and a function, H the choice of which are to be chosen to bring out an optimum solution. HAM has been applied to a wide variety of problems in different areas of science and technology.

The homotopy deformation equations for velocity u, micro-rotation $\mathcal{C}$ and temperature θ for both the zones are given by:

$$(1-q)L\left[u_i(y;q)-u_{i,o}(y)\right] = qh_u N_1[u_i(y;q)], \quad i = 1,2 \tag{20}$$

$$(1-q)L\left[\mathcal{C}_{i,o}(y;q)-\mathcal{C}_o(y)\right] = qh_{\mathcal{C}} N_2[\mathcal{C}_i(y;q)], \quad i = 1,2 \tag{21}$$

$$(1-q)L\left[\theta_{i,o}(y;q)-\theta_o(y)\right] = qh_\theta N_3[\theta_i(y;q)], \quad i = 1,2 \tag{22}$$

where $q \in [0,1]$ is the embedding homotopy parameter.

The auxiliary linear operator is chosen as:

$$L = \frac{d^2}{dy^2} \tag{23}$$

and non-linear differential operators N_1, N_2 and N_3 are expressions on LHS of equations for u, $\mathcal{C}$ and θ in (8)-(13).

The initial approximations of u(y), $\mathcal{C}(y)$ and $\theta(y)$ are chosen as $u_{1,0}$, $\mathcal{C}_{1,0}$, $\theta_{1,0}$ for Zone I and $u_{2,0}$, $\mathcal{C}_{2,0}$, $\theta_{2,0}$ for Zone II such that $L(u) = L(\mathcal{C}) = L(\theta)$ and satisfy the given boundary conditions (14)-(19). Hence these initial solutions are given by:

$$\begin{aligned} &u_1(y,0) = u_{1,0}(y) = 0, \quad \mathcal{C}_1(y,0) = \mathcal{C}_{1,0}(y) = 0, \quad \theta_1(y,0) = \theta_{1,0}(y) = \tfrac{n_k(y+1)}{1+n_k}, \\ &u_2(y,0) = u_{2,0}(y) = 0, \quad \mathcal{C}_2(y,0) = \mathcal{C}_{2,0}(y) = 0, \quad \text{and} \quad \theta_2(y,0) = \theta_{2,0}(y) = \tfrac{y+n_k}{1+n_k} \end{aligned} \tag{24}$$

The auxiliary parameters h_u, $h_{\mathcal{C}}$ and h_θ are assumed to be so selected that Equations (20)-(22) have solution at each point $q \in [0,1]$. With the help of Taylors series in q, u(y;q), $\mathcal{C}(y; q)$, $\theta(y; q)$ can be expressed as:

$$u_i(y;q) = \sum_{m=0}^{\infty} u_{i,m}(y) q^m, \quad i = 1,2 \tag{25}$$

$$\mathcal{C}_i(y;q) = \sum_{m=0}^{\infty} \mathcal{C}_{i,m}(y) q^m, \quad i = 1,2 \tag{26}$$

$$\theta_i(y;q) = \sum_{m=0}^{\infty} \theta_{i,m}(y) q^m, \quad i = 1,2 \tag{27}$$

When q = 1, Equations (20)-(22) are same as original Equations (8)-(13), respectively, therefore at $q = 1$ we get the exact solutions:

$$u_1(y,1) = u_1(y), \quad \mathcal{C}_1(y,1) = \mathcal{C}_1(y), \quad \theta_1(y,1) = \theta_1(y),$$

$$u_2(y,1) = u_2(y), \quad \mathcal{C}_2(y,1) = \mathcal{C}_2(y), \quad \theta_2(y,1) = \theta_2(y) \tag{28}$$

Therefore as q takes from 0 to 1, the solution $u_1(y;q)$ varies from initial guess $u_{1,0}(y)$ to the final (exact) solution $u_1(y)$. (This is similar for $\mathcal{C}_1(y)$,$\theta_1(y)$, u_2(y), $\mathcal{C}_2(y)$, $\theta_2(y)$). Later, the mth-order deformation equations are obtained by substituting (25)-(27) in Equations (20)-(22) and comparing the coefficient of q^m on both sides:

$$L\left[u_{i,m} - \mathrm{Y}_m u_{i,m-1}(y)\right] = h_u R^u_{i,m}(y) \tag{29}$$

$$L\left[\mathcal{C}_{i,m} - \mathrm{Y}_m \mathcal{C}_{i,m-1}(y)\right] = h_{\mathcal{C}} R^{\mathcal{C}}_{i,m}(y) \tag{30}$$

$$L\left[\theta_{i,m} - \mathrm{Y}_m \theta_{i,m-1}(y)\right] = h_\theta R^\theta_{i,m}(y) \tag{31}$$

with the homogeneous boundary conditions of:

$$u_{1,m}(-1) = 0, \quad u_{1,m}(1) = 0 \quad u_{1,m}(0^-) = u_{2,m}(0^+),$$

$$\left[\frac{\partial u_1}{\partial y}|(0^-) + 2c_1 \mathcal{C}_1|(0^-)\right] = n_\mu \left(\frac{1-c_1}{1-c_2}\right)\left[\frac{\partial u_2}{\partial y}|(0^+) + 2c_2 \mathcal{C}_2|(0^+)\right],$$

$$\mathcal{C}_{1,m}(-1) = 0, \quad \mathcal{C}_{1,m}(1) = 0, \quad \mathcal{C}_{1,m}(0^-) = \mathcal{C}_{2,m}(0^+), \quad \frac{d\mathcal{C}_{1,m}(0^-)}{dy} = n_\beta \frac{\mathcal{C}_{2,m}(0^+)}{dy}$$

$$\theta_{1,m}(-1) = 0, \quad \theta_{1,m}(1) = 0, \quad \theta_{1,m}(0^-) = \theta_{2,m}(0^+), \quad \frac{d\theta_{1,m}(0^-)}{dy} = n_k \frac{d\theta_{2,m}(0^+)}{dy} \tag{32}$$

where:

$$R^u_{1,m}(y) = \frac{d^2 u_{1,m-1}}{dy^2} + c_1 \frac{d\mathcal{C}_{1,m-1}}{dy} + \frac{Gr}{Re}(1-c_1)\theta_{1,m-1} Sin\varphi - (1-c_1)\mathrm{Re}\frac{dp}{dx} \tag{33}$$

$$R^{\mathcal{C}}_{1,m}(y) = \frac{d^2 \mathcal{C}_{1,m-1}}{dy^2} - s_1 \frac{du_{1,m-1}}{dy} - 2s_1 \mathcal{C}_{1,m-1} \tag{34}$$

$$R^{\theta}_{1,m}(y)=\frac{d^2\theta_{1,m-1}}{dy^2}+Br\left[\left[\sum_{n=0}^{m-1}\left(\frac{du_{1,n}}{dy}\frac{du_{1,(m-1)-n}}{dy}\right)+\left(\frac{c_1}{1-c_1}\right)\left(\sum_{n=0}^{m-1}\left(\frac{du_{1,n}}{dy}+2\mathcal{C}_{1,n}\right)\left(\frac{du_{1,(m-1)-n}}{dy}+2\mathcal{C}_{1,(m-1)-n}\right)\right)\right]+\delta_1\sum_{n=0}^{m-1}\left(\frac{d\mathcal{C}_{1,n}}{dy}\frac{d\mathcal{C}_{1,(m-1)-n}}{dy}\right)\right] \tag{35}$$

$$R^{u}_{2,m}(y)=\frac{d^2u_{2,m-1}}{dy^2}+c_2\frac{d\mathcal{C}_{2,m-1}}{dy}+\frac{Gr}{Re}\frac{n_b}{n_\mu}(1-c_2)\theta_{2,m-1}Sin\varphi-\frac{1}{n_\mu}Re\frac{dp}{dx} \tag{36}$$

$$R^{\mathcal{C}}_{2,m}(y)=\frac{d^2\mathcal{C}_{2,m-1}}{dy^2}-s_2\frac{du_{2,m-1}}{dy}-2s_2\,\mathcal{C}_{2,m-1} \tag{37}$$

$$R^{\theta}_{2,m}(y)=\frac{d^2\theta_{2,m-1}}{dy^2}+\frac{Br}{n_k}\left[n_\mu\left[\sum_{n=0}^{m-1}\left(\frac{du_{2,n}}{dy}\frac{du_{2,(m-1)-n}}{dy}\right)+\left(\frac{c_2}{1-c_2}\right)\left(\sum_{n=0}^{m-1}\left(\frac{du_{2,n}}{dy}+2\mathcal{C}_{2,n}\right)\left(\frac{du_{2,(m-1)-n}}{dy}+2\mathcal{C}_{2,(m-1)-n}\right)\right)\right]+n_\beta\,\delta_1\sum_{n=0}^{m-1}\left(\frac{d\mathcal{C}_{2,n}}{dy}\frac{d\mathcal{C}_{2,(m-1)-n}}{dy}\right)\right] \tag{38}$$

for m being integer $Y_m=0$, for $m\leqslant 1$ and $Y_m=1$, for $m>1$.

The m^{th}-order derivatives for $u(y;q)$, $\mathcal{C}(y;\ q)$, $\theta\ (y;\ q)$ are defined as $u_{i,m}(y)=(1/m!)\ ((\partial^m u_i(y;q))/(\partial q^m))$, $\mathcal{C}_{i,m}(y)=(1/m!)\ ((\partial^m \mathcal{C}_i(y;q))/(\partial q^m))$, $\theta_{i,m}(y)=(1/m!)\ \ ((\partial^m \theta_i(y;q))/(\partial q^m))$, i = 1,2.

Intrinsic to HAM is the assumption that the auxiliary linear operator (L) auxiliary parameter (h), and initial guess are chosen so that the above Taylor's series expansions are convergent at $q=1$(Misra and Ghosh, 2001). The effects of pertinent parameters on the flow of two immiscible incompressible micropolar fluids can be discussed from the exact solutions (25)-(27).

Heat transfer coefficient at the walls is given by Fourier's law $\overline{\mathbf{h}}=-k\nabla T$. In non-dimensional form this represents Nusselt number $Nu=-(d\theta/dy)]_{y=\pm 1}$. This is studied only at the walls of the channel.

4. Entropy generation analysis

4.1 The volumetric entropy generation

The non-equilibrium conditions due to the exchange of momentum and energy, within the fluid-fluid medium and at the solid boundaries, cause a continuous entropy generation in the flow field of the channel. This entropy generation is due to the irreversible nature of heat transfer and viscosity effects, within the fluid and at the

solid boundaries. From the known temperature and velocity fields, volumetric rate of entropy generation for incompressible micropolar fluid is given as:

$$(S_i)_G = (S_i)_{G,\text{heat transfer}} + (S_i)_{G,\text{viscous dissipation}} = \frac{k}{T_o^2}\left(\frac{\partial T}{\partial Y}\right)^2 + \frac{1}{T_o}\Phi$$

where Φ is the viscous dissipation function.

For the present study, the volumetric rate of entropy generation reduces to:

$$(S_i)_G = \underbrace{\frac{k_i}{T_o^2}\left(\frac{\partial T_i}{\partial Y}\right)^2}_{\geqslant 0} + \underbrace{\frac{\mu_i}{T_o}\left(\frac{\partial U_i}{\partial Y}\right)^2}_{\geqslant 0} + \underbrace{\frac{\kappa_i}{T_o}\left(\frac{\partial U_i}{\partial Y} + 2C_i\right)^2}_{\geqslant 0} + \underbrace{\frac{\beta_i}{T_o}\left(\frac{\partial C_i}{\partial Y}\right)^2}_{\geqslant 0} \tag{39}$$

where the value of i can be either 1 or 2 that represent fluid in Zone I and fluid in Zone II, respectively. Entropy generation profiles are constructed using Equation (39) when the velocity, micro-rotation and temperature fields are known in the medium. On the right hand side of the above equation the first term represents the entropy generation rate due to heat conduction and the remaining three terms represent the viscous dissipation function, Φ for an incompressible micropolar fluid.

4.2 The characteristic entropy generation rate

The characteristic entropy generation rate $S_{G,C}$ is defined as:

$$S_{G,C} = \left[\frac{(\overline{\mathbf{h}})^2}{k_1 T_o^2}\right] = \left[\frac{k_1(\Delta T)^2}{h^2 T_o^2}\right] \tag{40}$$

In the above equation, $\overline{\mathbf{h}}$ is the heat flux in Zone I, T_o is the average, characteristic, absolute reference temperature of the medium, $\Delta T = T_{II} - T_I$ and h is the half of transverse distance of the channel.

4.3 The entropy generation number

According to Bejan (1979), the dimensionless form of entropy generation is the entropy generation number *Ns* and which is, by definition, equal to the ratio of actual generation rate to a characteristic entropy transfer rate. The entropy generation number for each fluid with dimensionless variables is given by:

$$Ns_1 = \frac{(S_1)_G}{S_{G,C}} = \left(\frac{d\theta_1}{dy}\right)^2 + \frac{Br}{\Omega}\left[\left(\frac{du_1}{dy}\right)^2 + c_1\left(\frac{du_1}{dy} + 2\mathcal{C}_1\right)^2 + \delta_1\left(\frac{d\mathcal{C}_1}{dy}\right)^2\right] \tag{41}$$

$$Ns_2 = \frac{(S_2)_G}{S_{G,C}} = n_k\left(\frac{d\theta_2}{dy}\right)^2 + \frac{Br}{\Omega}\left[n_\mu\left(\left(\frac{du_2}{dy}\right)^2 + c_2\left(\frac{du_2}{dy} + 2\mathcal{C}_2\right)^2\right) + \delta_1 n_\beta\left(\frac{d\mathcal{C}_2}{dy}\right)^2\right] \tag{42}$$

where $Br = ((\mu_1 U_o^2)/k_1 \Delta T)$ is the Brinkman number, which determines the importance of viscous dissipation because of the fluid frictions relative to the

conduction heat flow resulting from the impressed temperature difference and $\Omega = (\Delta T/T_o)$ is the dimensionless temperature difference.

It is desirable to consider the Ec and Pr in a group that is called the Brinkman number ($Br = Ec$ .Pr) for evaluating the relative importance of the energy due to viscous dissipation to the energy because of heat conduction. It was reported that Br is much less than unity for many engineering processes (Bejan, 1979).

4.4 The viscous dissipation parameter

The viscous dissipation parameter is an important dimensionless number for the irreversibility analysis. It determines the relative importance of the viscous effects for the entropy generation and it is equal to the ratio of the Brinkman number to the dimensionless temperature difference, i.e., (Br/Ω).

4.5 Fluid friction vs heat transfer irreversibility

Entropy generation number (Ns) is good for generating entropy generation profiles but fails to give any idea about the relative importance of fluid friction and heat transfer effects. Two alternate parameters, irreversibility distribution ratio (ϕ) and Bejan number (Be), are introduced for this purpose and they are achieving increasing popularity among researchers studying the second law.

4.5.1 The irreversibility ratio. The idea of irreversibility distribution ratio can enhance the understanding of the irreversibilities associated with the heat transfer and the fluid friction. It is defined as the ratio of entropy generation due to fluid frictions (Nf) to heat transfer in the transverse direction (Ny), i.e.:

$$\phi = \frac{S_{G,\text{fluid friction}}}{S_{G,\text{heat transfer}}} = \left(\frac{Nf}{Ny}\right) \tag{43}$$

Here ϕ can be interpreted as follows: If $0 \leqslant \phi < 1$, then - indicates that heat transfer irreversibility dominates and if $\phi > 1$ the fluid friction dominates. For the case of $\phi = 1$, both the heat transfer and fluid friction have the same contribution to entropy generation.

4.5.2 The Bejan number. An alternative irreversibility distribution parameter (Paoletti *et al.*, 1989), called the Bejan number Be, was as the ratio of entropy generation due to heat transfer to the total entropy generation, is expressed as:

$$Be = \frac{Ny}{Ns} = \frac{Ny}{Ny+Nf} = \frac{1}{1+\phi} \tag{44}$$

This is employed to understand the entropy generation mechanisms. The value of $Be \to 1$ indicates that the heat transfer irreversibility dominates over fluid friction, and this corresponds to the case of $\phi \to 0$. On the other hand, $Be \to 0$ indicates that the irreversibility due to fluid friction dominates over the irreversibility due to the heat transfer. This corresponds to $\phi \to \infty$. It is obvious that $Be = 0.5$ is the case in which the irreversibility due to heat transfer is equal to fluid friction contributions in the entropy generation, and this corresponds to the case of $\phi = 1$.

5. Convergence of the HAM solution

5.1 h-curves

HAM provides us with a great freedom in choosing the solution of a non-linear problem by different base functions. This has a great effect on the convergence region because the convergence region and the rate of a series are chiefly determined by the base functions used to express the solution. Therefore, a non-linear problem could be approximated more efficiently by ensuring its convergency. The convergence and rate of approximation for the HAM solution depends on the value of auxiliary parameter h strongly. By means of the so-called h-curves, it is easy to find out the so-called valid regions of auxiliary parameters to gain a convergent series solution. The convergence and rate of approximation for the HAM solution depends on the value of auxiliary parameter h strongly. By means of the so-called h-curves, it is easy to find out the so-called valid regions of auxiliary parameters to gain a convergent series solution. The expressions for u, C and θ contain the auxiliary parameters h_u, h_C and h_θ. Here to see the admissible values of h_u, h_C and h_θ, the h-curves are plotted for 15th-order of approximation in Figure 2(a)-(c) by taking the values of the parameters as: $B = 0.2$, $Br = 0.1$, $c_1 = 0.3$, $c_2 = 0.3$, $\delta_1 = 0.1$, $Gr = 1.5$, $n_\beta = 0.9$, $n_k = 0.9$, $n_\mu = 0.9$, $n_\rho = 0.9$, $\varphi = \pi/4$, $Re = 2$, $s_1 = 2$ and $s_2 = 2$. It is clearly noted from Figure 2(a) that the range for the admissible values of h_u is $-0.95 < h_u < -0.7$. From Figure 2(b) it can be seen that the h_C curve has a line segment that corresponds to a region of $-0.9 < h_C < -0.4$. Figure 2(c) depicts that the admissible value of h_θ are $-1 < h_\theta < 0.2$. A wide valid zone is evident in these figures ensuring convergence of the series.

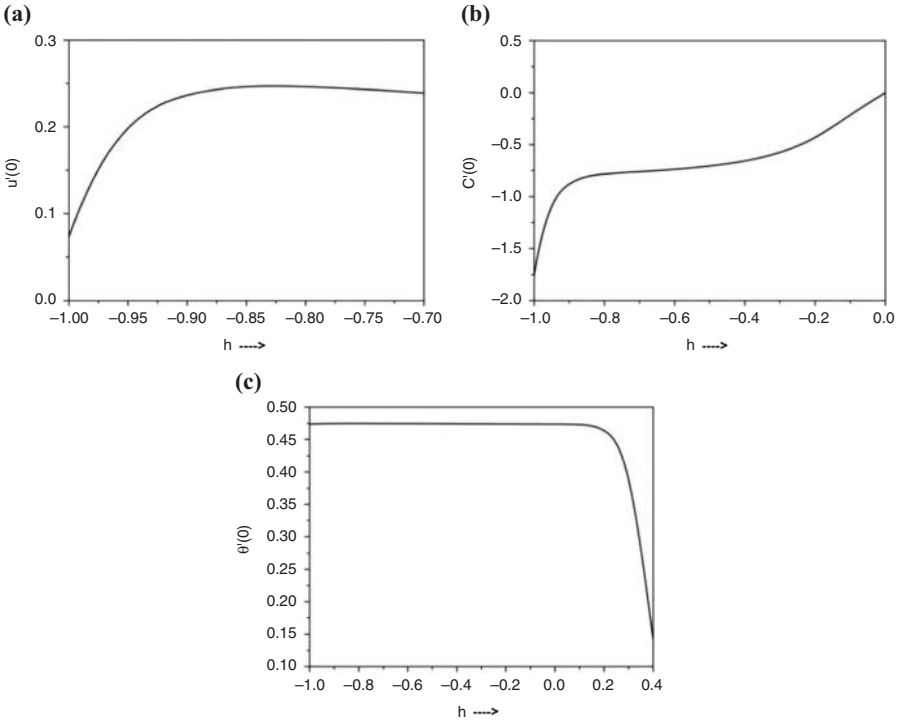

Figure 2.
The h-curves for velocity u(y), micro-rotation $C(y)$ and temperature θ(y)

6. Results and discussion

The solutions for $u_1, C_1, \theta_1, u_2, C_2$ and θ_2 have been computed and presented graphically through Figures 3(a)-11(b). The effects of various parameters like couples stress parameter, micropolarity parameter, Reynolds number, Grashof number and viscous dissipation parameter entering into the problem on velocity, micro-rotation, temperature, entropy generation number and Bejan number have been studied.

6.1 Effect of couple stress parameter (s_i)

From Figures 3(a)-(c) and 4(a)-(b), we notice that as couple stress parameter s_2 increases, velocity, temperature, entropy generation number and Bejan number increases. As couple stress parameter increases ($s_2 \to \infty$), i.e., couple stresses decreases ($\gamma \to 0$), we retrieve the case of a Newtonian fluid. Hence Figure 3(a) indicates that the velocity of the Newtonian fluid is more than that of the micropolar fluid. A part of velocity in micropolar fluids is due to couple stress tensor generated by rotation of particles. Hence we conclude that in one dimensional straight flow, the effect of couple stresses on velocity is small. From Figure 3(b) we see that the effect of couple stresses on micro-rotation is very high. As s_2 increases, micro-rotation increases. Hence we can say that couple stresses can affect micro-rotation very much. The temperature due to dissipation of energy (depending on velocity) also changes very slightly. This is seen in Figure 3(c) as s_2 increases temperature increases slightly. The same effect is seen on the entropy generation number Ns in Figure 4(a). But near

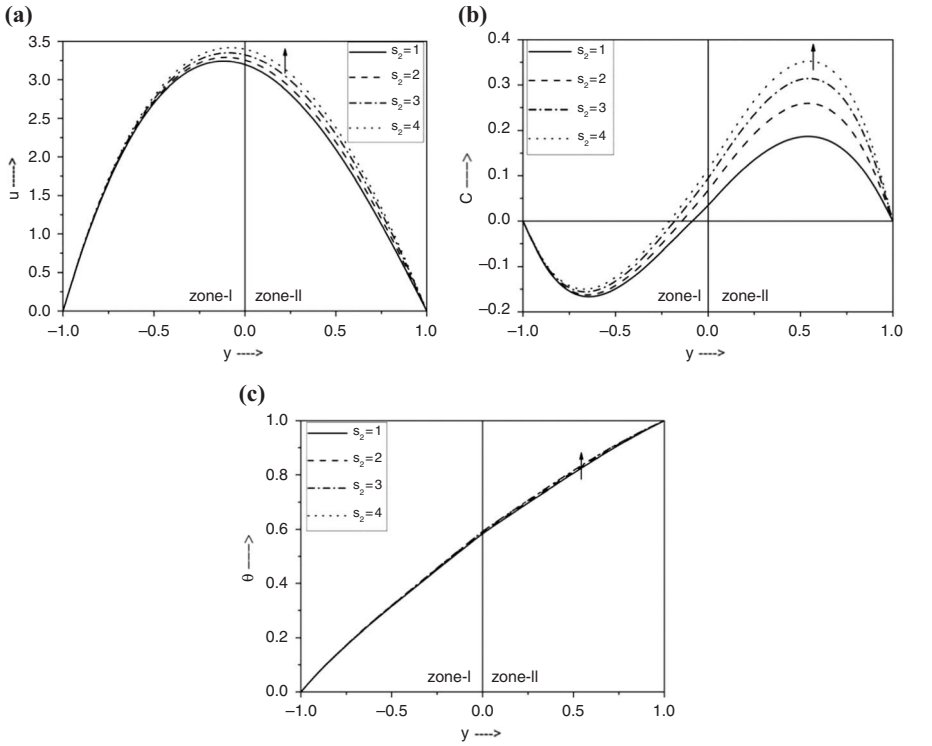

Figure 3.
Variation of non-dimensional (a) velocity; (b) micro-rotation; and (c) temperature profiles for various values of s_2 with fixed values of $B = -0.6$, $Br = 0.1$, $c_1 = 0.6$, $c_2 = 0.6$, $\delta_1 = 0.1$, $Gr = 0.8$, $n_\beta = 0.8$, $n_k = 1.2$, $n_\mu = 0.9$, $n_\rho = 0.9$, $\varphi = \pi/4$, $Re = 2$, $s_1 = 2$

the plates effect of couple stresses on Ns is considerable. This may be due to more friction near the walls. From Figure 4(b) we see that Bejan number is higher at the interface. From the limiting case of $s_2 \to \infty$, we see that Be for viscous fluids is less than the micropolar fluids. A slight increase in couple stress parameter s_2, increases Bejan number Be very much at the interface. Since Be is nearly zero near to the plates, the entropy generation rate in the transverse direction is almost zero (at upper plate) and fluid friction dominates.

6.2 Effect of cross-viscosity or micropolarity parameter (c_i)

From Figures 5(a)-(c) and 6(a)-(b), we observe that as micropolarity parameter c_2 increases, velocity (considerably), micro-rotation (numerically), temperature and entropy generation number decreases. But Bejan number Be increases. As $c_2 \to 0$, we retrieve the case of Newtonian viscous fluid. As c_2 increases, it is observed from Figure 5(a) that velocity decreases. The velocity in case of micropolar fluid is less compared to that of viscous fluid case. In Figure 6(a), the variation of the entropy generation number *Ns* is shown, which varies in entire region of *y* with variation in c_2 is shown. We observe that *Ns* is minimum at the interface and variation in $c_2$will not affect *Ns* but c_2 effects Ns very much near the plates. The opposite behavior is seen in the case of Bejan number Be (Figure 6(b)). As c_2 increases, *Be* also increases. This is in contrast to the behavior of *Ns* as s_2 increases. We see that *Be* at any point y is more than 0.4 near the plates. This indicates that even near to the walls effect of friction is low. This is a very useful property. We can conclude that micropolarity of fluids reduces the frictional effects near the plates.

6.3 Effect of Reynolds number (Re)

From Figures 7(a)-(c) and 8(a)-(b), we observe that as the Reynolds number Re increases, the velocity, micro-rotation (numerically), temperature and entropy generation number *Ns* are increases. All these values of u, C, θ and *Ns* rise very much with a small raise in the Re values. But near the walls Bejan number decreases as Re increases which shows high dissipation of energy or entropy generation rate near the plates. But near the walls Bejan number decreases as Re increases which shows high dissipation of energy or entropy generation rate near the plates. From Figure 8(a),

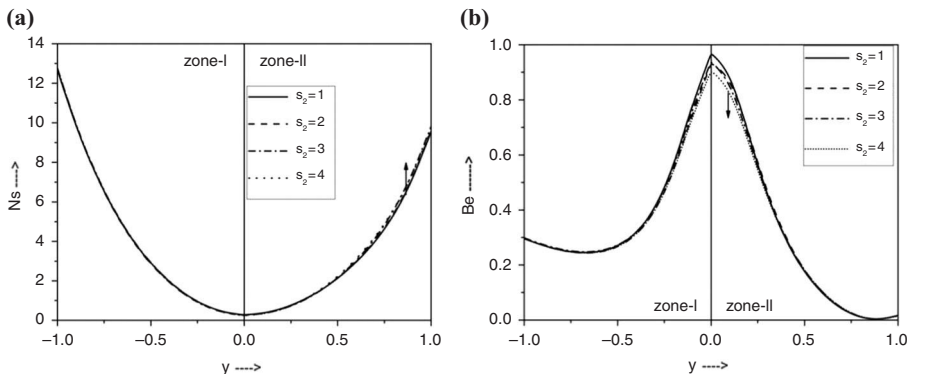

Figure 4. Variation of non-dimensional (a) entropy generation number; (b) Bejan number for various values of s_2 with fixed values of B = –0.1, Br = 0.8, $c_1 = 0.1$, $c_2 = 0.1$, $\delta_1 = 0.1$, Gr = 2, $n_\beta = 0.9$, $n_k = 1$, $n_\mu = 0.9$, $n_\rho = 0.9$, $\varphi = \pi/4$, Re = 2, $s_1 = 1$, $\Omega = 1$

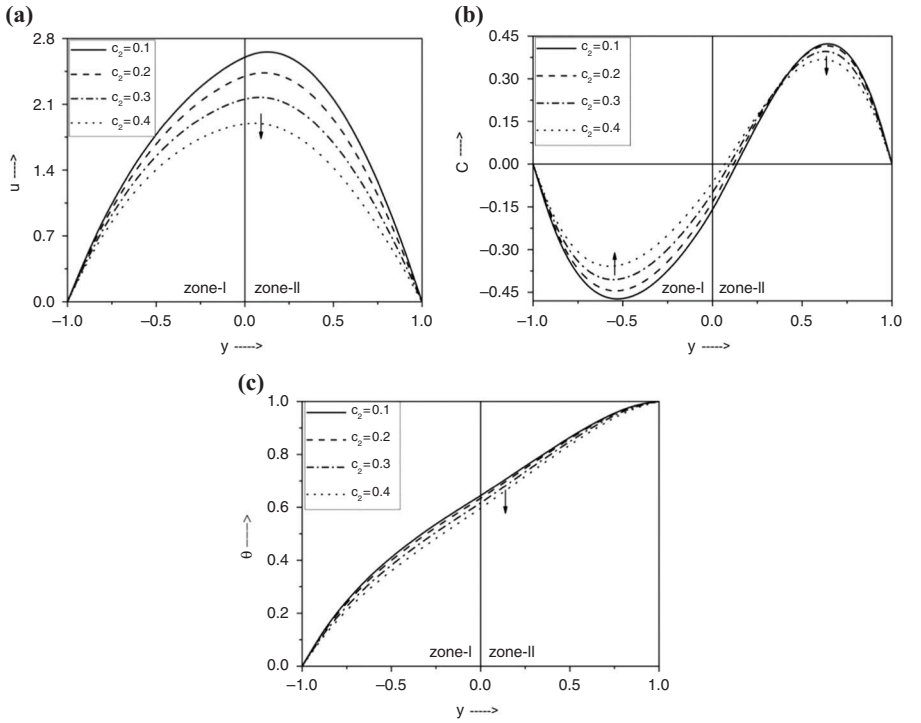

Figure 5.
Variation of non-dimensional (a) velocity; (b) micro-rotation; and (c) temperature profiles for various values of c_2 with fixed values of $B = -0.3$, $Br = 0.1$, $c_1 = 0.8$, $\delta_1 = 0.1$, $Gr = 1.2$, $n_\beta = 0.9$, $n_k = 0.9$, $n_\mu = 0.9$, $n_\rho = 0.9$, $\varphi = \pi/4$, $Re = 2$, $s_1 = 2$, $s_2 = 2$

Figure 6.
Variation of non-dimensional (a) entropy generation number; (b) Bejan number for various values of c_2 with fixed values of $B = -0.1$, $Br = 0.1$, $c_1 = 0.4$, $\delta_1 = 0.5$, $Gr = 0.1$, $n_\beta = 0.9$, $n_k = 1$, $n_\mu = 0.9$, $n_\rho = 0.9$, $\varphi = \pi/4$, $Re = 2$, $s_1 = 1$, $s_2 = 1$, $\Omega = 1$

it is observed that the linear temperature distribution between the two plates occurs at a low value of the Reynolds number ($Re = 1$). This linear temperature profile corresponds to the energy due to heat conduction is dominant over the energy due to viscous dissipation. Also from Figure 8(a), it is observed that the larger velocity and temperature gradients occurring near the plates enhance the entropy generation in those regions.

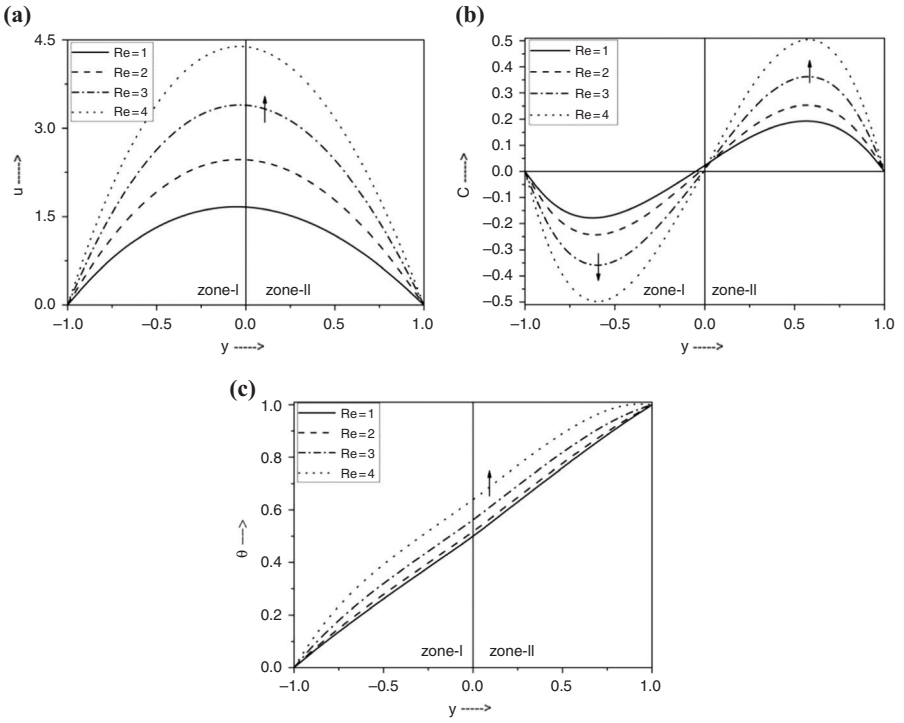

Figure 7.
Variation of non-dimensional (a) velocity; (b) micro-rotation; and (c) temperature profiles for various values of Re with fixed values of $B = -0.3$, $Br = 0.1$, $c_1 = 0.5$, $c_2 = 0.5$, $\delta_1 = 0.1$, $Gr = 1.2$, $n_\beta = 0.9$, $n_k = 0.9$, $n_\mu = 0.9$, $n_\rho = 0.9$, $\varphi = \pi/4$, $s_1 = 2$, $s_2 = 2$

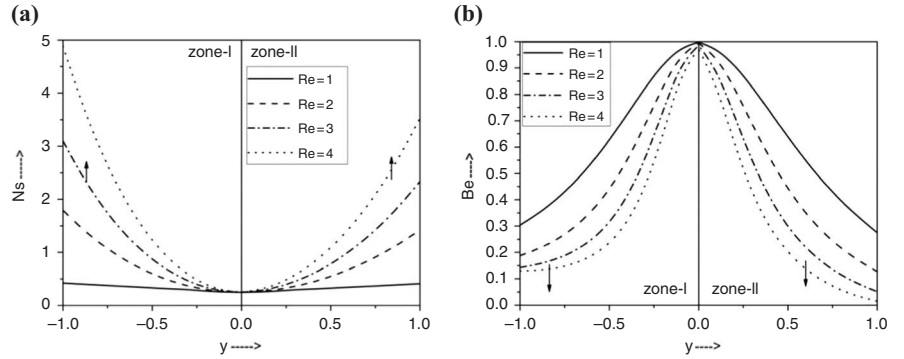

Figure 8.
Variation of non-dimensional (a) entropy generation number; (b) Bejan number for various values of Re with fixed values of $B = -0.1$, $Br = 0.1$, $c_1 = 0.2$, $c_2 = 0.2$, $\delta_1 = 0.2$, $Gr = 0.8$, $n_\beta = 0.9$, $n_k = 1$, $n_\mu = 0.9$, $n_\rho = 0.9$, $\varphi = \pi/4$, $s_1 = 1$, $s_2 = 1$, $\Omega = 1$

6.4 Effect of Grashof number (Gr)

From Figures 9(a)-(c) and 10(a)-(b) we notice that as the Grashof number *Gr* increases, velocity, micro-rotation, temperature and entropy generation number increases. Figure 9(a) indicates that the effect of Grashof number on velocity is high. From Figure 9(b)-(c), we observe that as *Gr* increases, micro-rotation and temperature

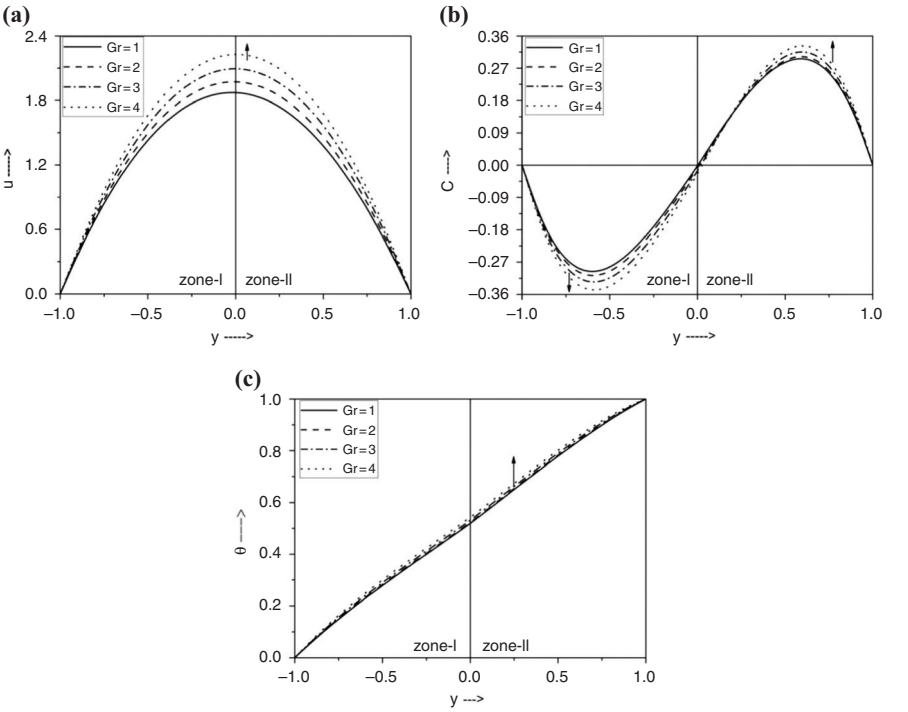

Figure 9.
Variation of non-dimensional (a) velocity; (b) micro-rotation; and (c) temperature profiles for various values of Gr with fixed values of $B = -0.3$, $Br = 0.1$, $c_1 = 0.2$, $c_2 = 0.2$, $\delta_1 = 0.1$, $n_\beta = 0.9$, $n_k = 0.9$, $n_\mu = 0.9$, $n_\rho = 0.9$, $\varphi = \pi/4$, $Re = 1$, $s_1 = 2$, $s_2 = 2$

Figure 10.
Variation of non-dimensional (a) entropy generation number; (b) Bejan number for various values of Gr with fixed values of $B = -0.2$, $Br = 0.1$, $c_1 = 0.3$, $c_2 = 0.3$, $\delta_1 = 0.2$, $n_\beta = 0.9$, $n_k = 1$, $n_\mu = 0.9$, $n_\rho = 0.9$, $\varphi = \pi/4$, $s_1 = 1$, $Re = 2$, $s_1 = 2$, $s_2 = 1$, $\Omega = 1$

increases slightly. The same effect is seen on entropy generation number *Ns* in Figure 10(a). But near the plates effect of Grashof number on *Ns* is considerable. This may be due to more friction near the walls. From Figure 10(b) we see that Bejan number is higher at the interface. As Grashof number *Gr* increases, Bejan number *Be* very much at the interface.

6.5 Effect of viscous dissipation parameter (Br/Ω)

The effect of the viscous dissipation parameter (Br/Ω) on the entropy generation number *Ns* and Bejan number *Be* are shown in Figures 11(a)-(b). A small raise in the values of (Br/Ω), increases the values of entropy generation number Ns and decreases the values of Bejan number *Be* very much. At a low value of (Br/Ω), the entropy generation number is independent of the transverse distance, which corresponds to the energy due to heat conduction and is dominant over the energy because of viscous dissipation since the viscous dissipation parameter measures the relative importance of the entropy generation due to the viscous effect to temperature gradient. There is a lowest point of the entropy generation at each specified value of the viscous dissipation parameter except for the value of $(Br/\Omega) = 0$. At the high values of the (Br/Ω), each plate acts as a strong concentrator of irreversibility due to the high velocity and temperature gradients occurring near the plates. The figures indicate that at the interface $y = 0$, the entropy generation rate is minimum, i.e., available energy in transverse direction at the interface is maximum. At the plates *Be* is minimum and *Ns* is maximum, i.e., the fluid friction dominates near the plates.

From Figures 4(b) and 6(b), the comparative study of effect of couple stress parameter s_2 and micropolarity parameter c_2 on Be shows that near the plates s_2 has no effect but c_2 increases the values of *Be*. Again we observe that Be is more than 0.4 near the walls for c_2 and Be is almost zero near the walls for s_2 in Figures 4(b) and 6(b). This indicates that micropolarity parameter offers smoothness to the walls and hence friction near the walls deceases. This shows an industrial application that micropolar fluids with high micropolarity and less couples stresses will act as a good lubricant. The reason for this may be due to the fact that much of the momentum of the fluid particles is transferred to the rotation of the particles by decreasing their velocity. Hence friction and dissipation of energy decreases near the plates.

7. Conclusion

In this paper, the flow of two incompressible immiscible micropolar fluids between two inclined parallel plates has been studied. The governing equations are expressed in the non-dimensional form and are solved by using HAM. The second law of thermodynamics is applied to investigate the irreversibilities in terms of the entropy generation rate. The effect of viscous dissipation parameter or group parameter (Br/Ω)

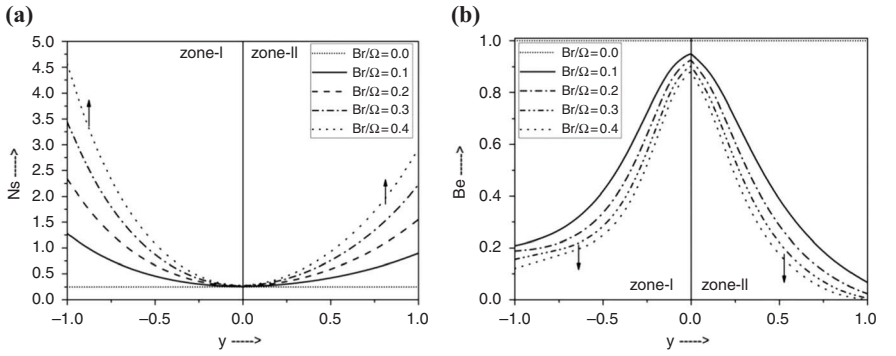

Figure 11. Variation of non-dimensional (a) entropy generation number; (b) Bejan number for various values of (Br/Ω) with fixed values of $B = -0.1$, $c_1 = 0.1$, $c_2 = 0.1$, $\delta_1 = 0.2$, $Gr = 0.5$, $n_\beta = 0.9$, $n_k = 1$, $n_\mu = 0.9$, $n_\rho = 0.9$, $\varphi = \pi/4$, $s_1 = 2$, $s_2 = 2$

on the entropy generation number (*Ns*), Bejan number (*Be*) is presented through figures. It is observed that:

(1) The presence of couple stresses in the fluid increases the velocity and temperature.

(2) The presence of micro-rotation decreases the velocity in comparison with the Newtonian fluid case.

(3) The temperature distribution at low values of the Reynolds number and Grashof number is found to be a linear function of y between the two plates, while it is found to be a non-linear function of y at larger values of those parameters.

(4) The entropy generation distribution is not independent of the velocity and the temperature distributions. When the value of $(Br/\Omega) = 0$, the entropy generation distribution is observed to be independent of the transverse distance and the entropy generation increases with increasing the viscous dissipation parameter (Br/Ω) at certain constant values of other parameters.

(5) The entropy generation rate is maximum near the plates in both the zones as compared to that of the channel interface. This demonstrates that the frictional forces are dominant near the plates and these forces enhance the entropy production. Conversely, Bejan numbers have minimum values neat to the plates and maximum values near to the interface.

(6) The entropy generation rate is more near the plate in Zone I than that of Zone II. This may be due to the fact that the fluid in Zone I is more viscous. This indicates the more the viscosity of the fluid is, the more the entropy generation.

(7) Bejan number is a maximum at the centre point of the channel. This reveals that the amount of available energy for work is more and irreversibility is less.

(8) Based on limiting values of micropolarity parameter $(c \to 0)$ and couple stress parameter $(s \to \infty)$, we conclude that the values of velocity, temperature and entropy generation number for viscous fluid are more than the corresponding values in micropolar fluid case. This may be due to the fact that in viscous fluids micro-rotations are absent this implies that exergy is not transformed to give micro-rotation to the particles and hence velocity, etc. increases and hence entropy increases.

(9) As micropolarity increases, entropy generation rate near the plates decreases and irreversibility decreases. This indicates an important industrial application for micropolar fluids to use them as a good lubricant.

References

Bakhtiyarov, S.I. and Siginer, D.A. (1997), "A note on the laminar core-annular flow of two immiscible fluids in a horizontal tube", *Proceeding International Symposium on Liquid-Liquid Two Phase Flow and Transport Phenomena, Begell House, Inc., Santa Barbara, CA*, pp. 107-111.

Baytas, A.C. (2000), "Entropy generation for natural convection in an inclined porous cavity", *International Journal of Heat and Mass Transfer*, Vol. 43 No. 12, pp. 2089-2099.

Bejan, A. (1979), "A study of entropy generation in fundamental convective heat transfer", *Journal of Heat Transfer*, Vol. 101 No. 4, pp. 718-725.

Bejan, A. (1982), "Second-law analysis in heat transfer and thermal design", *Advances in Heat Transfer*, Vol. 15, pp. 1-58.

Bejan, A. (1996), *Entropy Generation Minimization*, CRC Press, Boca Raton, NY.

Bhattacharyya, K., Mukhopadhyay, S., Layek, G.C. and Pop, I. (2012), "Effects of thermal radiation on micropolar fluid flow and heat transfer over a porous shrinking sheet", *International Journal of Heat and Mass Transfer*, Vol. 55 Nos 11-12, pp. 2945-2952.

Chamkha, A.J. (2000), "Flow of two immiscible fluids in porous and nonporous channels", *Journal of Fluids Engineering*, Vol. 121 No. 1, pp. 117-124.

Chamkha, A.J. (2004), "Oscillatory flow and heat transfer in two immiscible viscous fluids", *International Journal of Fluid Mechanics Research*, Vol. 31 No. 1, pp. 13-36.

Eringen, A.C. (1966), "The theory of micropolar fluids", *Journal of Mathematics and Mechanics*, Vol. 16, pp. 1-18.

Eringen, A.C. (2001), *Microcontinnum Field Theories-II: Fluent Media*, Springer, New York, NY.

Giamberini, M., Amendola, E. and Carfagna, C. (1997), "Lightly crosslinked liquid crystalline epoxy resins: the effect of rigid-rod length and applied stress on the state of order of the cured thermoset", *Macromolecular Chemistry and Physics*, Vol. 198 No. 10, pp. 3185-3196.

Havzali, M., Arikoglu, A., Komurgoz, G., Keser, H.I. and Ozkol, I. (2008), "Analytical-numerical analysis of entropy generation for gravity-driven inclined channel flow with initial transition and entrance effects", *Physica Scripta*, Vol. 78 No. 4, Article No. 045401.

Hayakawa, H. (2000), "Slow viscous flows in micropolar fluids", *Physical Review E*, Vol. 61 No. 5B, pp. 5477-5492.

Jena, S.K. and Mathur, M.N. (1981), "Similarity solutions for laminar free convection flow of a thermo-micropolar fluid past a non-isothermal vertical flat plate", *International Journal of Engineering Science*, Vol. 19 No. 11, pp. 1431-1439.

Kiwan, S. and Khodier, M. (2011), "Natural convection heat transfer in an open-ended inclined channel-partially filled with porous media", *Heat Transfer Engineering*, Vol. 29 No. 1, pp. 67-75.

Kolpashchikov, V., Migun, N.P. and Prokhorenko, P.P. (1983), "Experimental determination of material micropolar fluid constants", *International Journal of Engineering Science*, Vol. 21 No. 4, pp. 405-411.

Komurgoz, G., Arikoglu, A., Turker, E. and Ozkol, I. (2010), "Second law analysis for an inclined channel containing porous-clear fluid layers by using the differential transform method", *Numerical Heat Transfer, Part A: Applications. An International Journal of Computation and Methodology*, Vol. 57 No. 8, pp. 603-623.

Kumar, J.P., Umavathi, J.C., Chamkha, A.J. and Pop, I. (2010), "Fully developed free convective flow of micropolar and viscous fluids in a vertical channel", *Applied Mathematical Modelling*, Vol. 35 No. 5, pp. 1175-1186.

Liao, S.J. (1992), "The proposed homotopy analysis technique for the solution of nonlinear problems", PhD thesis, Shanghai Jiao Tong University, Shanghai.

Liao, S.J. (2003), *Beyond Perturbation: Introduction to Homotopy Analysis Method*, Chapman and Hall-CRC Press, Boca Raton, FL.

Lukaszewicz, G. (1999), *Micropolar Fluids: Theory and Applications*, Birkhauser, Boston, MA.

Malashetty, M.S. and Umavathi, J.C. (1997), "Two phase magnetohydrodynamic flow and heat transfer in an inclined channel", *International Journal of Multiphase Flow* , Vol. 23 No. 3, pp. 545-560.

Malashetty, M.S., Umavathi, J.C. and Kumar, J.P. (2004), "Two fluid flow and heat transfer in an inclined channel containing porous and fluid layer", *Heat and Mass Transfer*, Vol. 40 No. 11, pp. 871-876.

Migun, N.P. (1981), "Experimental method of determining parameters characterizing the microstructure of micropolar fluids", *Journal of Engineering Physics and Thermophysics*, Vol. 41 No. 2, pp. 832-835 (translated from Inzhenerno-Fizicheskii Zhurnal, Vol. 41, pp. 220-224, 1983).

Misra, J.C. and Ghosh, S.K. (2001), "A mathematical model for the study of interstitial fluid movement vis-a-vis the non-Newtonian behaviour of blood in a constricted artery", *Computers & Mathematics with Applications*, Vol. 41 Nos 5-6, pp. 783-811.

Paoletti, S., Rispoli, F. and Sciubba, E. (1989), "Calculation exergetic loses in compact heat exchanger passages", *ASME AES*, Vol. 10 No. 2, pp. 21-29.

Rees, D.A.S. and Bossom, A.P. (1996), "The Blasius boundary layer flow of a micropolar fluid", *International Journal of Engineering Science*, Vol. 34 No. 1, pp. 113-124.

Su, W.F.A., Chen, K.C. and Tseng, S.Y. (2000), "Effects of chemical structure changes on thermal, mechanical, and crystalline properties of rigid rod epoxy resins", *Journal of Applied Polymer Science*, Vol. 78 No. 2, pp. 446-451.

Turk, M.A., Sylvester, N.D. and Ariman, T. (1973), "On pulsatile blood flow", *Journal of Rheology*, Vol. 17 No. 1, pp. 1-21.

Umavathi, J.C., Chamkha, A.J. and Shekar, M. (2014), "Flow and heat transfer of two micropolar fluids separated by a viscous fluid layer", *International Journal of Microscale and Nanoscale Thermal and Fluid Transport Phenomena*, Vol. 5 No. 1, pp. 23-49.

Umavathi, J.C., Chamkha, A.J. and Sridhar, K.S.R. (2010), "Generalized plain Couette flow and heat transfer in a composite channel", *Transport in Porous Media*, Vol. 85 No. 1, pp. 157-169.

Umavathi, J.C., Chamkha, A.J. and Veershetty, S. (2012), "Fully developed mixed convection of a micropolar fluid in a vertical channel with boundary conditions of third kind", *International Journal of Energy & Technology*, Vol. 4 No. 1, pp. 1-9.

Umavathi, J.C., Kumar, J.P. and Chamkha, A.J. (2008), "Flow and heat transfer of a micropolar fluid sandwiched between viscous fluid layers", *Canadian Journal of Physics*, Vol. 86 No. 8, pp. 961-973.

Umavathi, J.C., Kumar, J.P. and Chamkha, A.J. (2009a), "Convective flow of two immiscible viscous and couple stress permeable fluids through a vertical channel", *Turkish Journal of Engineering and Environmental Sciences*, Vol. 33 No. 4, pp. 221-243.

Umavathi, J.C., Chamkha, A.J., Manjula, M.H. and Al-Mudhaf, A. (2005a), "Flow and heat transfer of a couple stress fluid sandwiched between viscous fluid layers", *Canadian Journal of Physics*, Vol. 83 No. 7, pp. 705-720.

Umavathi, J.C., Chamkha, A.J., Manjula, M.H. and Al-Mudhaf, A. (2005b), "Magneto-convection of a two-fluid flow through a vertical channel", *International Journal of Heat and Technology*, Vol. 23 No. 5, pp. 151-163.

Umavathi, J.C., Chamkha, A.J., Mateen, A. and Al-Mudhaf, A. (2005c), "Unsteady two-fluid flow and heat transfer in a horizontal channel", *Heat and Mass Transfer*, Vol. 42 No. 1, pp. 81-90.

Umavathi, J.C., Chamkha, A.J., Mateen, A. and Al-Mudhaf, A. (2009b), "Unsteady oscillatory flow and heat transfer in a horizontal composite porous medium channel", *Nonlinear Analysis: Modelling and Control*, Vol. 14 No. 3, pp. 397-415.

Umavathi, J.C., Kumar, J.P., Chamkha, A.J. and Pop, I. (2005d), "Mixed convection in a vertical porous channel", *Transport in Porous Media*, Vol. 61 No. 3, pp. 315-335.

Umavathi, J.C., Mateen, A., Chamkha, A.J. and Al-Mudhaf, A. (2006), "Oscillatory Hartmann two-fluid flow and heat transfer in a horizontal channel", *International Journal of Applied Mechanics and Engineering*, Vol. 11 No. 1, pp. 155-178.

Further reading

Makinde, O.D. (2006), "Irreversibility analysis for gravity driven non-Newtonian liquid film along an inclined isothermal plate", *Physica Scripta*, Vol. 74 No. 6, pp. 642-645.

Saouli, S. and Aiboud-Saouli, S. (2004), "Second law analysis of laminar falling liquid film along an inclined heated plate", *International Communications in Heat and Mass Transfer*, Vol. 31 No. 6, pp. 879-886.

Turkyilmazoglu, M. (2011), "Numerical and analytical solutions for the flow and heat transfer near the equator of an MHD boundary layer over a porous rotating sphere", *International Journal of Thermal Sciences*, Vol. 50 No. 5, pp. 831-842.

Corresponding author

Ali J. Chamkha can be contacted at: achamkha@pmu.edu.sa